ELECTROSTATIC DEFLECTOR OF THE CYCLOTRON DC-280 AXIAL INJECTION CHANNEL

N.Kazarinov#, I.Ivanenko, FLNR, JINR, Dubna, Russia

Abstract

The spherical electrostatic deflector will be used in the axial injection channel of the DC-280 cyclotron for rotation of the ion beam onto vertical axis. The results of the simulation of beam dynamics in the deflector based on 3D electrical field map are discussed in this report. The results of simulation of the ion beam transport in the axial injection beam line of the cyclotron are presented also.

INTRODUCTION

The isochronous heavy-ion cyclotron DC-280 is a basic part of the Super Heavy Element Facility – the new accelerator complex of Joint Institute for Nuclear Research [1,2]. The DC-280 cyclotron will produce high-intensity beam of accelerated ions in the range from helium to uranium. The maximum design value of a current of ion beams will be 10 pmcA and the maximum kinetic energy will be 8 MeV/u.

In this report the design of the spherical electrostatic deflector of high voltage injection system [2, 3] of DC-280 cyclotron is presented. Using the electrostatic deflector is explained both weight reduction and lower power of the power supply system in comparison with the bending magnet. The design is based on three-dimensional calculation of the electric field carried out by using OPERA 3D program code [4].

The 3D macro-particle beam dynamic simulation in the deflector was done in the curvilinear coordinates system connected with reference orbit, defined for computational field map. This simulation was carried out by using MCIB04 program code [5].

3D PHYSICAL MODEL OF DEFLECTOR

3D physical model of electrostatic deflector is shown in Fig. 1.

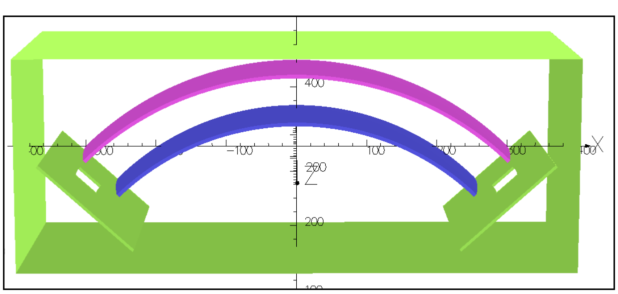

Figure 1: Physical model of deflector.

Bender consists of two electrodes under the potentials U_1 (blue colour), U_2 (red colour) and three ground electrodes (green colour). The design bending radius R=40 cm, the gap between the electrodes d = 6 cm, the horizontal width of the electrodes h = 16 cm. The electric field map consists of two distributions $\Phi_{1,2}(\vec{r})$ corresponding to the following combinations of voltages at the electrodes (U_1=-10kV,U_2=0) and (U_1=0,U_2=10kV). The resulting field map of the deflector $\Phi(\vec{r})$ is a superposition of these distributions:

$$\Phi(\vec{r}) = \left[U_2\Phi_2(\vec{r}) - U_1\Phi_1(\vec{r})\right]\times 10^{-4} \qquad (1)$$

The distributions of the components $E_{X,Y}$ of the electric field along the designed orbit of the deflector are shown in Fig.2.

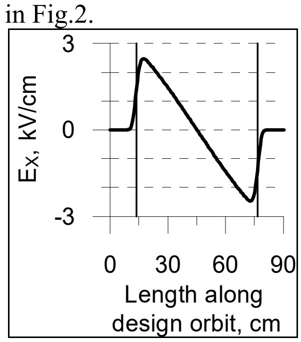

Figure 2a: E_X component of electric field.

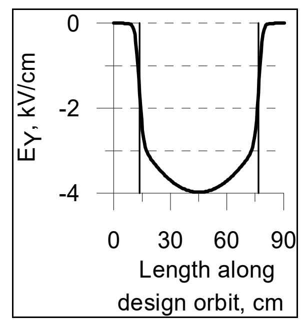

Figure 2b: E_Y component of electric field.

CALCULATED EQUILIBRIUM ORBIT

The calculated equilibrium (solid line) and design (dashed line) orbits are shown in Fig.3a. Deviation Δ between calculated and designed orbits is shown in Fig.3b. In the non-relativistic approximation, the equilibrium orbit in the deflector does not depend on the mass-to-charge ratio A/Z of the ion.

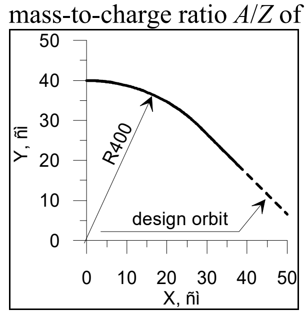

Figure 3a: Deflector orbits.

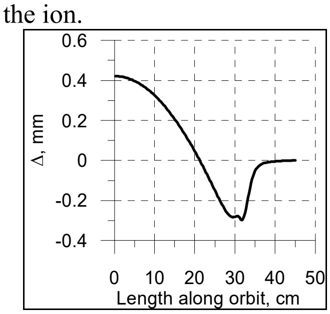

Figure 3b: Deviation Δ .

The particle motion at the equilibrium orbit of the deflector is completely determined by two functions – the curvature of the orbit $K_0(s)$ and "friction coefficient" $\Lambda_0(s)$:

#nyk@lnr.jinr.ru

ISBN 978-3-95450-131-1

$$K_0(s) = -\frac{E_n(s)}{(B\rho\beta)_0}\,;\; \Lambda_0(s) = \frac{E_t(s)}{(B\rho\beta)_0} \qquad (2)$$

Where s – is the distance along the equilibrium orbit; $E_{n,t}(s)$ – are normal and tangent components of the electric field at the equilibrium orbit; $B\rho_0$ and β_0 – are magnetic rigidity and relativistic velocity of the reference particle, respectively.

BEAM FOCUSING IN THE DEFLECTOR

The simulation of the dynamics of the ions in the deflector is convenient to carry out in the natural system of the coordinate (*x,z,s*) associated with calculated equilibrium orbit. The equation for the radius of the particle $\vec{r}$ in this coordinate system has a form (prime denotes the differentiation with respect to *s*):

$$\vec{r}\,'' = \left(\frac{V'}{V} - \frac{V_0'}{V_0}\right)\vec{r}\,' + \frac{1}{B\rho\beta}\left[\left(\frac{V}{V_0}\right)^2 \vec{E} - \left(\vec{r}\,'\vec{E}\right)\vec{r}\,'\right]$$
$$(B\rho\beta)' = [2 - \beta_0^2 (V/V_0^2)](\vec{r}\,'\vec{E}) \qquad (3)$$
$$\frac{V}{V_0} = \sqrt{(1+K_0 x)^2 + x'^2 + z'^2}$$

The linear approximation of the equations of motion (3) determines the focusing properties of the deflector:

$$x'' = -\Lambda_0 x' - (3-\beta_0^2)K_0^2 x + \frac{1}{(B\rho\beta)_0}\frac{\partial E_n}{\partial x}x +$$
$$+2\frac{\Delta M}{M_0}K_0 \;;\; z'' = -\Lambda_0 z' + \frac{1}{(B\rho\beta)_0}\frac{\partial E_z}{\partial z}z \qquad (4)$$
$$(\Delta M/M_0)(B\rho\beta)_0 = const$$

The derivatives of components of the electric field in equation (4) should be evaluated at the equilibrium orbit with the help of the field map. The variable $\Delta M/M_0$ connects with momentum deviation $\Delta p/p_0$ of the ion:

$$\Delta M/M_0 = \Delta p/p_0 + K_0 x \qquad (5)$$

Let us consider the focusing property of the commonly used spherical and cylindrical deflectors.

Spherical Deflector

In the case of ideal spherical deflector we have:

$$K_0 = \frac{1}{R}\,;\; \Lambda_0 = 0\,;\; \frac{\partial E_n}{\partial x} = -2\frac{E_n}{R}\,;\; \frac{\partial E_z}{\partial z} = \frac{E_n}{R}$$
$$x'' = -\frac{1-\beta_0^2}{R^2}x + \frac{2}{R}\frac{\Delta M}{M_0}\,;\; z'' = -\frac{1}{R^2}z\,;\; \frac{\Delta M}{M_0} = (\frac{\Delta p}{p_0})_{in} \qquad (6)$$

Here $(\Delta p/p_0)_{in}$ – is the momentum spread at the entrance of the deflector. In accordance with equations (6) the focusing terms are approximately the same both for x- and z- motions.

Cylindrical Deflector

In the case of ideal cylindrical deflector we have:

$$K_0 = \frac{1}{R}\,;\; \Lambda_0 = 0\,;\; \frac{\partial E_n}{\partial x} = -\frac{E_n}{R}\,;\; \frac{\partial E_z}{\partial z} = 0$$
$$x'' = -\frac{2-\beta_0^2}{R^2}x + \frac{2}{R}\frac{\Delta M}{M_0}\,;\; z'' = 0\,;\; \frac{\Delta M}{M_0} = (\frac{\Delta p}{p_0})_{in} \qquad (7)$$

The focusing term is absent for z- motion.

Edge Field

The simulation of the beam focusing in the field map of the spherical deflector by using the linear equations (4) shows the significant asymmetry of the beam envelopes at the exit of the deflector. This asymmetry is caused by edge field and may be minimized by shifting the equilibrium orbit towards the inner electrode of the deflector. The entrance and the exit points of the orbit do not changed during this shifting.

In this regime the magnitude of the voltage at the electrodes are $U_1 \cong$-16 kV and $U_2 \cong$10 kV in the case of maximum injection voltage U_{inj} = 80 kV. The maximum deviation of the calculated equilibrium orbits from the design one is about 8 mm. The difference between x- and z-envelopes at the exit of deflector is less than 1mm.

Beam Transport through Deflector

The macro particle simulation of the ion beam transport through the deflector by using equation of motion (3) verified the possibility of the correction of the beam focusing asymmetry. The beam envelopes and the beam emittance during transportation are shown in Fig.4.

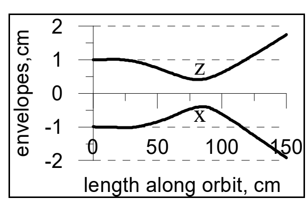

Figure 4a: Beam envelopes.

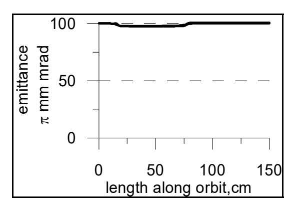

Figure 4b: Beam emittance.

The ion distributions at various phase planes in the final point of transportation are shown in Fig.5.

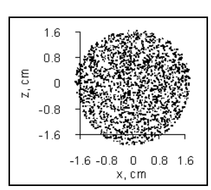

Figure 5a: Plane (x,z).

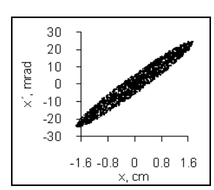

Figure 5b: Plane (x,x′).

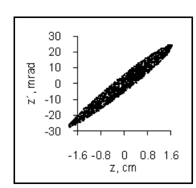

Figure 5c: Plane (z,z′).

ISBN 978-3-95450-131-1

As may be seen from Fig.5 in the "shifted orbit" regime the beam is almost axial symmetric. The influence of the nonlinearity of the electric field is negligibly small.

DC-280 AXIAL INJECTION CHANNEL

The scheme of the high voltage axial injection beam line of DC-280 cyclotron is shown in Fig.6.

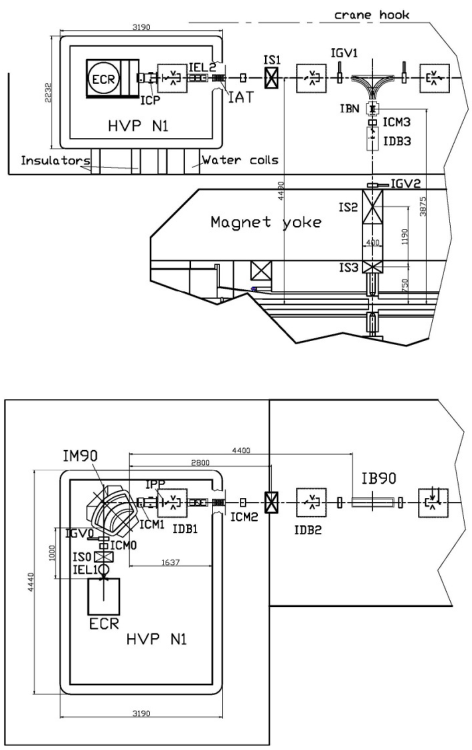

Figure 6: Scheme of axial injection channel. HVP – High Voltage Platform; ECR – ECR ion source; IS0-3 – focusing solenoids; IM90 – analyzing magnet; IEL1,2 electrostatic lenses; IAT – acceleration tube; IBD90 – spherical electrostatic deflector.

The ion beam is extracted from ECR ion source with energy 25 keV/Z. After analyzing and separation in the IM90 magnet the beam is accelerated in IAT tube. The kinetic beam energy may be increased by acceleration up to 80 keV/Z. All these equipment is placed at High Voltage Platform HVP. The electrostatic deflector IB90 rotates the beam onto vertical axis and two solenoids IS2,3 match the beam emittance with acceptance of the cyclotron inflector.

In the numerical simulation of the ion beam dynamics in the axial injection beam line 3D field maps of analyzing magnet IM90 [6], solenoids IS0-3, acceleration tube IAT and spherical electrostatic deflector IB90 are used.

The transport of $^{48}Ca^{8+}$ ion beam with kinetic energy of 75 keV/Z was considered. The dependence of the beam envelopes on length along the channel are shown in Fig.7.

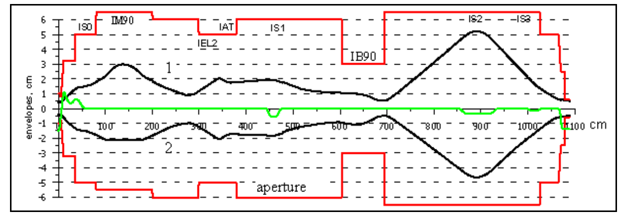

Figure 7: Horizontal (curve 1) and vertical (curve 2) $^{48}Ca^{8+}$ ion beam envelopes.

The horizontal (red curve) and vertical (blue curve) beam emittances are shown in Fig.8. The decreasing of the beam emittance is explained by increasing of kinetic energy in the acceleration tube IAT.

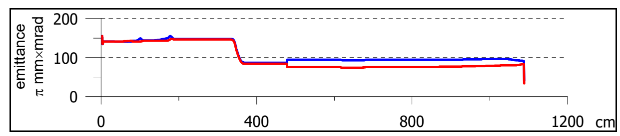

Figure 8: $^{48}Ca^{8+}$ ion beam emittances.

The efficiency of the beam transport is equal to 100%.

REFERENCES

[1] G.Gulbekyan, B.Gikal, I.Kalagin, N.Kazarinov. "Status Report and Future Development FLNR JINR Heavy Ions Accelerators Complex", Proceedings of 11-th International Conference on Heavy Ion Accelerators Technology, HIAT09, 8-12 June 2009, Venezia, Italy, p.p. 59-63.

[2] I.Ivanenko, G.Gulbekyan, N.Kazarinov, E.Samsonov, "Injection and Acceleration of Intense Heavy Ion Beams in JINR New Cyclotron DC280", MOA1C02, these proceedings, HIAT 2015, Yokohama, Japan (2015).

[3] G.G. Gulbekyan, V. Bekhterev, S.L. Bogomolov, A.A. Efremov, B. Gikal, I.A. Ivanenko, I.V. Kalagin, N.Yu. Kazarinov, M.V. Khabarov, V.N. Melnikov, N.F. Osipov, S.V. Prokhorov, A. Tikhomirov, "The Project of the HV Axial Injection for the DC-280 Cyclotron at the FLNR JINR", Proceedings of XXIV Russian Accelerator Conference, RuPAC'2014, Obninsk, Russia (2014), p.p. 333-335.

[4] OPERA-3D Reference Manual, Oxford OX5 1JE, England, October 2012

[5] V.Alexandrov, N.Kazarinov, V.Shevtsov, "Multi-Component Ion Beam code – MCIB04". Proceeding of XIX-th Russian Particle Accelerator Conference, RUPAC2004, 4-9 October, Dubna, Russia, p.p.201-203.

[6] N.Yu.Kazarinov, I.A.Ivanenko, "Magnets of Injection and Extraction Systems of Cyclotron DC280". Proceedings of XXIV Russian Accelerator Conference, RuPAC'2014, Obninsk, Russia (2014), p.p. 339-341.

ISBN 978-3-95450-131-1